Wood Science and Technology (2024) 58:273–293
https://doi.org/10.1007/s00226-023-01513-2

ORIGINAL

Improving the flame retardancy of furfurylated wood by introducing DOPO

Youming Dong[1,4] · Zhenyu Fu[1] · Yutao Yan[2] · Jingbo Shi[1] · Mark Hughes[3] · Xianxu Zhan[4] · Jianzhang Li[1]

Received: 4 April 2023 / Accepted: 9 November 2023 / Published online: 29 December 2023

Abstract

Poor dimensional stability, sensitivity to microorganisms, and flammability restrict the application of wood in certain areas where these properties are critical. Although furfurylation can improve the physical and mechanical properties of wood, the heat and smoke release of furfurylated wood during combustion are dramatic and need to be addressed. As a kind of halogen-free phosphorus flame retardant, 9,10-dihydro-9-oxa-10-phosphaphenanthrene-10-oxide (DOPO) and its derivatives exhibit excellent performance in polymer composites. In this study, DOPO was dissolved in furfuryl alcohol (FA) and used to modify wood. The effect of DOPO on the thermal stability, combustion behavior, and physical and mechanical properties of furfurylated wood was investigated. The chemical structure, morphology, and char residue after combustion were also characterized. The studies show that DOPO can react with the FA polymer and is incorporated and homogeneously dispersed in the wood structure. Compared to untreated wood, furfurylated wood has a much higher heat and smoke release during combustion. The addition of DOPO remarkably reduces the heat release of furfurylated wood, and this effect increases as the amount of DOPO increases. When the amount of introduced DOPO of furfurylated wood is 7%, its total heat release is reduced by 37.4% and becomes comparable to the untreated wood. However, DOPO does not suppress smoke production effectively. DOPO improves the thermal stability of furfurylated wood by promoting char formation and inhibiting the diffusion of oxygen and the escape of pyrolysis products. The addition of DOPO has little effect on the physical and mechanical properties of furfurylated wood. The results indicate that the combination of DOPO and furfurylation could be an efficient way to prepare highly stable and fire-resistant wood materials.

Extended author information available on the last page of the article

Introduction

As an indispensable raw material, wood is ubiquitously used in furniture, decoration, construction, and tools owing to its good processability, excellent mechanical properties, and pleasant aesthetic appearance (Dong et al. 2019). In recent decades, the depletion of fossil resources and growing environmental concerns have led to increasing demand for wood, since it is both renewable and biodegradable (Buonocore et al. 2014). However, for some applications, wood has some inherent drawbacks, such as its dimensional instability, occasionally poor mechanical properties, sensitivity to microorganisms, and flammability, which need to be addressed before it can be more widely utilized.

Hygroscopicity is the predominant issue; this results in the swelling and shrinkage of wood under changing levels of ambient relative humidity and can lead to deformation and cracking (Ouyang et al. 2022). In addition, water in wood provides a favorable environment for microorganisms (fungi, blue stain, and mold) and insects, which lead to wood degradation and a reduction in strength (Grinins et al. 2021; Žlahtič-Zupanc et al. 2018). Strenuous attempts have been made to improve the water resistance of wood (Hill 2006). Among the many methods that have been developed, furfurylation has been well researched and commercialized; it is an environmentally friendly method that improves dimensional stability through its bulking effect and hydrophobicity by the introduction of furfuryl alcohol (FA) into the wood cell wall and its subsequent in situ polymerization (Dong et al. 2020b; Esteves et al. 2011; Li et al. 2020; Yang et al. 2022). In addition to the formation of a cross-linked network, covalent bonds between the furan polymers and the wood components (mainly lignin) may be formed (Barsberg and Thygesen 2017; Ehmcke et al. 2017). Meanwhile, the hardness and stiffness of wood, along with its resistance to biodegradation are also improved (Hadi et al. 2021; Martin et al. 2021; Thygesen et al. 2021; Zhang et al. 2022a).

It has also been confirmed that furfurylation has a positive effect on the thermal stability of wood, albeit the total heat release and total smoke production during wood combustion are still dramatic (Dong et al. 2015). This offers interesting further possibilities, though additional flame retardancy is generally required. Some environmentally friendly flame-retardant materials, such as montmorillonite (Zhang et al. 2022b) and ammonium dihydrogen phosphate (Kong et al. 2018), have been incorporated into the furfurylation system to cause a synergistic effect, increasing the flame retardancy of wood. However, the poor interaction between polymer and inorganic salts can lead to the leaching of the latter from the wood (Marney and Russell 2008). The incorporation of inorganic nanoparticles also faces difficulties regarding dispersion and penetration into the wood (Samanta et al. 2022). It is, therefore, highly desirable to find a simple and stable method for improving the flame retardancy of furfurylated wood.

Compounds containing halogens, phosphorous, boron, and nitrogen have been identified as being effective components in flame retardants. However, due to the adverse effects on humans and the environment, halogenated flame retardants have been restricted in the wood industry. Nitrogen phosphorus-based

flame retardants, which could redirect decomposition reactions in favor of reactions yielding char residues and reducing the amount of combustible gases, have received more attention (Dhumal et al. 2022; Jiang et al. 2015; Lu et al. 2021). As halogen-free phosphorus flame retardants, 9,10-dihydro-9-oxa-10-phosphaphenanthrene-10-oxide (DOPO) and its derivatives have attracted much attention in the flame-retardant research community because of their versatile flame extinguishing behavior (Salmeia and Gaan 2015). Many studies have reported the use of DOPO to enhance the flame retardancy of polymers, such as epoxy resins, poly (lactic acid), polyesters, and polyamides (Cao et al. 2021; Jin et al. 2019; Kundu et al. 2020; Zhang et al. 2021; Zhou et al. 2021). The flame-retardant mechanism of DOPO can be explained by the release of low molecular weight phosphorus-containing compounds, arising from the breakage of the phosphaphenanthrene group, promoting the dehydration of polymers, and forming a phosphorus-rich thick char (Qian et al. 2011).

Given the excellent results obtained in polymers, some studies have attempted to improve the flame retardancy of wood-based products by grafting the DOPO onto wood fibers or incorporating it in the formulation of flame-retardant coatings (Ma et al. 2019; Thomas et al. 2021). However, limited research has been undertaken using DOPO as a fire retardant to modify solid wood. DOPO, being insoluble in water, generally requires the use of volatile and toxic organic solvents to impregnate wood. Moreover, the chemical reaction between wood and DOPO is difficult to achieve, resulting in poor durability and volatilization of DOPO prior to combustion (Weng et al. 2016). Fortunately, FA can readily dissolve DOPO, facilitating its impregnation into the wood structure. Meanwhile, the stability of DOPO in wood may be improved by the blanketing effect of the FA polymer and the possible reaction between the phosphaphenanthrene group and unsaturated C=C bonds in the FA polymer (Qiu et al. 2013). Therefore, the combination of DOPO and FA could be an efficient way of simultaneously endowing wood with good dimensional stability, flame retardancy, and durability.

In the present study, the feasibility of the combined modification of solid wood using DOPO and FA was explored. The reaction mechanism of DOPO and FA was investigated and the dimensional stability, mechanical properties, and flame retardancy of the resulting modified wood, with different content of DOPO were evaluated. The chemical changes, micromorphology, and char residue of wood were also characterized to analyze the flame-retardant mechanisms of the combined modification.

Experimental

Materials

Furfuryl alcohol (FA, 97% purity), 9,10-dihydro-9-oxa-10-phosphaphenanthrene-10-oxide (DOPO, 97% purity), and maleic anhydride (99% purity) were purchased from Shanghai Macklin Biochemical Co., Ltd. Dimethyl sulfoxide-*d*6 (DMSO-*d*6) was purchased from Shanghai Aladdin Biochemical Technology Co., Ltd and used

as the NMR solvent. Fast-growing poplar (*Populus tomentosa* Carr.) wood with a density of 0.38 g/cm^3 was machined into specimens with dimensions of 100 mm (longitudinal) × 100 mm (tangential) × 10 mm (radial) and 150 mm (longitudinal) × 10 mm (tangential) × 10 mm (radial). All samples were oven-dried at 103 °C to a constant weight and stored in a desiccator.

Modification of wood

FA solutions with 1% maleic anhydride and 0, 2%, 5%, and 7% DOPO were prepared by directly dissolving maleic anhydride and DOPO in FA (Table S1). The wood samples were immersed into these solutions under vacuum at − 0.1 MPa for 30 min and soaked at atmospheric pressure for 12 h. All impregnated samples were cured at 100 °C for 10 h and oven-dried at 105 °C until reaching constant weight. According to the amount of DOPO (0, 2%, 5%, and 7%), the treated wood samples were labeled as FA, FA-2DOPO, FA-5DOPO, and FA-7DOPO, respectively.

Characterization of FA-DOPO polymer

The FA polymers in the absence or presence of DOPO were prepared via polymerization catalyzed by maleic anhydride (100 °C for 10 h). The weight ratio of FA and DOPO was 3:1. The cured polymers were ground into 200-mesh powder and analyzed by Fourier transform infrared spectroscopy (FTIR, Thermo Scientific Nicolet iS20, USA) and X-ray photoelectron spectroscopy (XPS, Thermo Fisher Scientific K-Alpha + XPS system, USA). ^{1}H-NMR and ^{31}P-NMR spectra were carried out to clarify the structure of FA-DOPO polymers by using a Bruker AVANCE 400 NMR spectrometer (Bruker, Switzerland). The thermal stability of FA-DOPO polymers was analyzed by a thermogravimetric analyzer (TGA55, TA Instruments, USA) from room temperature to 800 °C with a heating rate of 10 °C/min under nitrogen and oxygen atmospheres.

Characterization of modified wood

The modified wood samples were separately ground into powder, passed through a 200-mesh sieve and analyzed by FTIR (Thermo Scientific Nicolet iS20, USA) and XPS (Thermo Fisher Scientific K-Alpha + XPS system, USA). The microstructure and elemental distribution of the untreated and treated wood were observed by a Field-emission scanning electron microscope (FE-SEM, Hitachi Regulus 8100, Japan) with energy-dispersive X-ray spectroscopy (EDX). The char residue after a cone calorimetry test was also analyzed by SEM–EDX to explore the fire-retardant mechanism. The accelerating voltage of the SEM was 3 kV.

Cone calorimetry was carried out using a TCC cone calorimeter (NETZSCH TAURUS Instruments GmbH, Germany) according to the ISO 5660–1 standard. Each of the wood samples (100 × 100 × 10 mm^3) was wrapped in aluminum foil and irradiated with an external heat flux of 50 kW/m^2. The parameters including the heat release rate (HRR), total heat release (THR), smoke production rate (SPR), total

smoke release (TSR), time to ignition (TTI), maximum average rate of heat emitted (MARHE), and effective heat of combustion (EHC) were recorded. Two replicates in each group were tested.

8–10 mg of powdered wood samples was tested in a thermogravimetric analyzer (TGA55, TA Instruments, USA) from room temperature to 600 °C at a heating rate of 10 °C/min under nitrogen and oxygen atmospheres.

Measurement of physical and mechanical properties

After modification, all samples were dried at 105 °C until they reached constant weight. The weight percent gain (WPG) was calculated as follows:

$$\mathrm{WPG}(\%) = \frac{m_1 - m_0}{m_0} \times 100$$

where m_0 and m_1 are the oven-dried weight of a sample before and after modification, respectively.

The samples (10 replicates in each group) were immersed in deionized water at room temperature and the weight was taken after different time intervals (1, 2, 4, 7 and 10 days). The water uptake (WU) was expressed as follows:

$$\mathrm{WU}(\%) = \frac{m_4 - m_3}{m_3} \times 100$$

where m_3 and m_4 are the weight of a sample before and after water immersion, respectively.

For dimensional stability, the dimensions of the samples (10 replicates in each group) were measured after 10-days water immersion. The volumetric swelling (S) and mean anti-swelling efficiency (ASE) were calculated as follows:

$$\mathrm{S}(\%) = \frac{V_1 - V_0}{V_0} \times 100$$

$$\mathrm{ASE}(\%) = \frac{S_0 - S_1}{S_0} \times 100$$

where V_0 and V_1 denote sample volume before and after water immersion, respectively. S_0 is volumetric swelling of an untreated sample, and S_1 is that of a treated sample.

The samples (10 replicates in each group) were leached with water, changed daily. After 10 days, all samples were dried at 105 °C and weighted. The leachability was calculated as follows:

$$\mathrm{Leachability}(\%) = \frac{m_5 - m_6}{m_5} \times 100$$

where m_5 and m_6 are the oven-dried weight of a sample before and after water leaching, respectively.

The dynamic contact angles on the surfaces of wood samples parallel to the grain were recorded with an DSA100 contact angle apparatus (KRÜSS GmbH, Hamburg, Germany). A 3 μL drop of deionized water was placed on the wood surface (planed by 1–2 mm before testing) using a micro-syringe. The average value was obtained as a total of at least five replicates.

The modulus of rupture (MOR) and modulus of elasticity (MOE) of all oven-dried untreated and treated samples (10 replicates in each group) were tested using a universal testing machine (AGS-X10KN, Shimadzu, Japan) under three-point bending, according to Chinese standards GB/T 1936.1–2009 and GB/T 1936.2–2009, respectively. The loading rate was 10.0 mm/min. Before testing, all sample dimensions were measured using digital calipers with a precision of 0.01 mm.

Hardness was measured using a TH210 durometer (Beijing TIME High Technology Ltd., China) and expressed as Shore D hardness according to ASTM D2240 method. Twenty tests were performed on each kind of sample.

Results and discussion

Reaction mechanism of FA and DOPO

In the first part of this study, the FA polymers in the absence or presence of DOPO were prepared via a polymerization route catalyzed by maleic anhydride. The XPS spectrum of FA-DOPO polymer displays an increase in the P2p peak compared with that of the FA polymer (Fig. 1a, b). FTIR was used to characterize the DOPO and the as-obtained FA polymers, as shown in Fig. 1c. The absorption peaks of DOPO appear at 3061 (Ph-H), 2433 (P–H), 1238 (P=O), and 755 cm^{-1} (P–O–Ph) (Peng

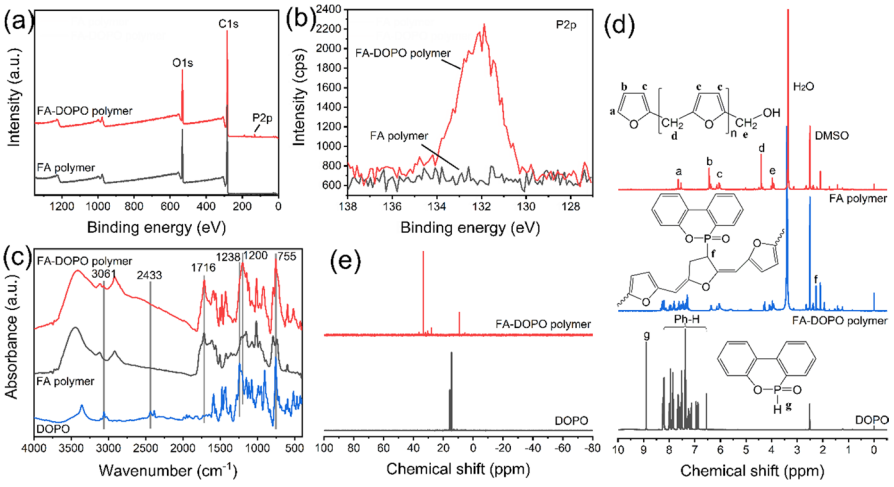

Fig. 1 Characterization of DOPO and FA polymers in the absence or presence of DOPO: **a** full scan XPS spectra, **b** high-resolution XPS spectra of P2p, **c** FTIR spectra, **d** ^{1}H-NMR and **e** ^{31}P-NMR spectra. The covalent bond is formed between FA polymer and DOPO

et al. 2021; Wang and Zhang 2004). In the spectrum of the FA-DOPO polymer, peaks at 3061 and 755 cm^{-1} are observed, implying the successful incorporation of DOPO into the FA polymer. Notably, the peak at 2433 cm^{-1} disappeared while the peak at 1238 cm^{-1} shifted to 1200 cm^{-1}. These results indicate that there was a substitution reaction between the FA polymer and DOPO.

To further clarify the reaction mechanism of the FA polymer and DOPO, NMR tests were carried out and the proton spectra are shown in Fig. 1d. After polymerization, FA can form a black thermoset polymer with cross-linked and conjugated chemical structures (Kherroub et al. 2015; Principe et al. 2000). The main signals observed in the FA polymer protons are consistent with previous studies (Kherroub et al. 2015; Ünver and Öktem 2013). In the spectrum of the FA-DOPO polymer, the chemical shift of the P–H signal at around 8.9 ppm in DOPO disappears, aligned with the FTIR results, suggesting the successful incorporation and reaction of DOPO with the FA polymer. Meanwhile, a new chemical shift is observed at 2.26 ppm, which could be related to the formation of a P–C bond between DOPO and the FA polymers. During the FA polymerization, polycondensation is the first reaction that forms linear FA oligomers with an unsaturated structure. Then, the cross-linking reaction could occur between two linear chains through Diels–Alder reaction (Falco et al. 2018). The possible reaction between DOPO and the FA polymer is the P–H bond of DOPO with C = C derived from the FA unsaturated structures. An inferred structure of the bonding is displayed in Fig. 1d. As a result, the chemical shift of ^{31}P-NMR spectrum for DOPO is also changed in the FA-DOPO polymer (Fig. 1e). However, the exact reaction mechanism between DOPO and the FA polymer would need to be further clarified using model compounds due to the complex reaction routes of the FA polymer under different conditions.

The effect of DOPO on the thermal degradation behavior of the FA polymer was evaluated using TGA analysis, as shown in Fig. 2. Under nitrogen atmosphere,

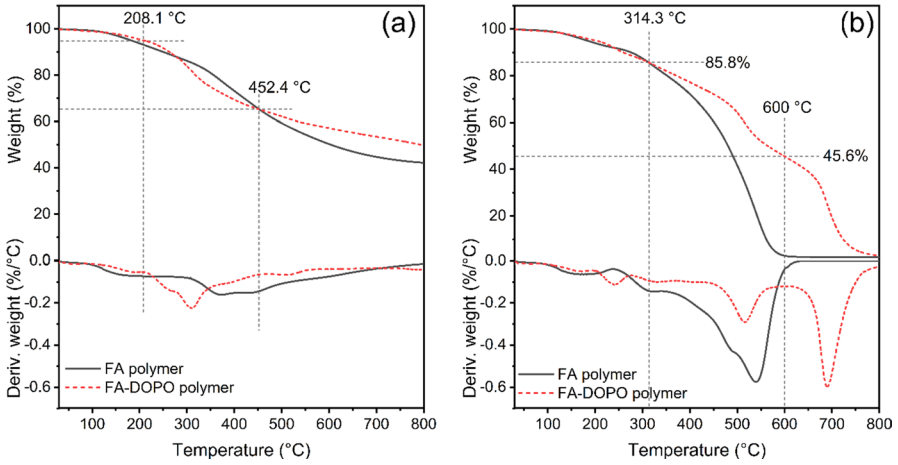

Fig. 2 TGA and dTG curves of the FA polymer in the absence or presence of DOPO in **a** nitrogen and **b** oxygen atmosphere. The addition of DOPO has a positive effect in improving the thermal stability of the FA polymer

the addition of DOPO promotes the thermal degradation of polymer between 208 – 452 °C. Afterward, the degradation rate of FA-DOPO polymer is lower than that of the FA polymer, which results in an increased char residue from 42 to 50%. Under an oxygen atmosphere, it is noted that the thermo-oxidative degradation process of the FA polymer mainly occurs between 314 – 600 °C, corresponding to the fracture and degradation of the cross-linking FA network. The onset of degradation of the FA-DOPO polymer is also at 314 °C. However, the weight loss between 314 – 600 °C is 40%, much lower than that of the FA polymer (83%). Notably, an additional degradation stage above 600 °C appears in the curve of the FA-DOPO polymer. These results indicate that DOPO can promote char formation of the FA polymer and inhibit the oxidative degradation of the char formed at higher temperatures, thus improving the thermal stability of the FA polymer.

Chemical and microstructure of the untreated and treated wood

After treatment, all samples exhibited high WPG values ranging from 134 to 139% (Fig. 3), indicating successful furfurylation and suggesting that the effect of DOPO addition on WPG was negligible. In addition, the surface color of all furfurylated wood samples became dark redish-brown (Fig. S1).

The chemical structure of the treated and untreated wood samples was investigated by FTIR, and the spectra ranging from 400 to 2000 cm^{-1} are shown in Fig. 4. After furfurylation, new peaks related to the FA polymer in all treated wood samples are visible. The peak at 1716 cm^{-1} is associated with the C=O in diketone structures (Bertarione et al. 2019). The peaks at 1562 and 790 cm^{-1} are attributed to C=C stretching and C-H wagging of the 2,5-subsituted furan ring, respectively (Pin et al. 2015). The peaks at 1014, 740 and 596 cm^{-1} are attributed to furan rings (Yao et al. 2005). The characteristic peaks originating from the DOPO structure are not evident

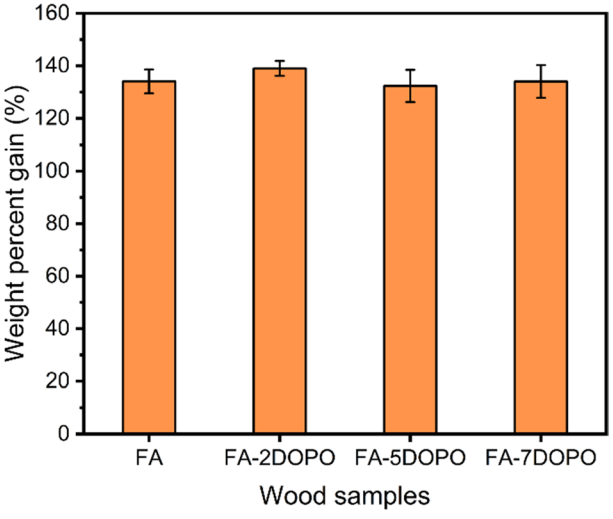

Fig. 3 Weight percent gain (WPG) of furfurylated wood with different concentration of DOPO

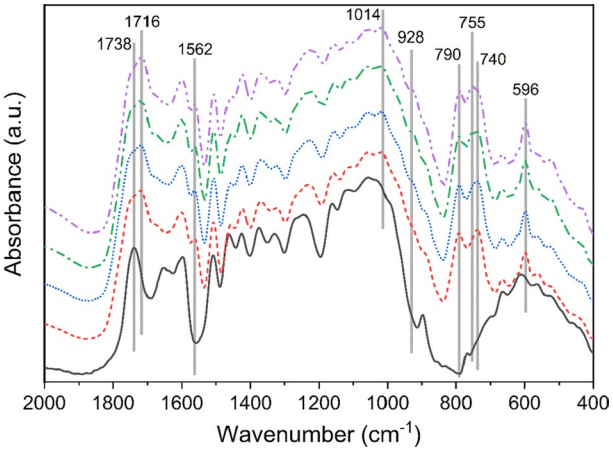

Fig. 4 FTIR spectra of untreated and treated wood samples

due to the signal overlapping and low content of DOPO. However, two weak peaks at 928 and 755 cm^{-1} (P–O–Ph) are observed. They are enhanced with an increase in DOPO concentration (Wang and Zhang 2004), indicating the successful incorporation of DOPO into the furfurylated wood.

The microstructure of treated and untreated wood samples is shown in Fig. 5. Obviously, large parts of the wood cell lumens are filled with polymer after furfurylation. In addition, the wood cell walls are thicker than that of untreated wood, suggesting that impregnation of the cell walls has been successful. As the concentration of DOPO increases, the atomic percentage of phosphorus in wood samples increases from 0.56% to 1.28% (Fig. 5f and Fig. S2). To analyze the distribution of DOPO in the wood structure, the elements carbon, oxygen, and phosphorus in the FA-7DOPO sample were scanned with EDX. Due to the FA polymer filling both the wood cell wall and lumen, the carbon and oxygen elements derived from the wood and FA polymers are distributed uniformly in the cross-section of the FA-7DOPO sample (Fig. 5g, h). The uniform distribution of phosphorus is also identified (Fig. 5i), indicating the homogeneous dispersion of DOPO within the wood structure.

Thermal stability of the untreated and treated wood

Figure 6 shows the TG and dTG curves of untreated and treated wood samples, and detailed data are listed in Table 1. T_{max} is defined as the temperature at the maximum weight loss rate in each degradation stage. Under a nitrogen atmosphere, the thermal degradation of all wood samples occurs mainly between 200 °C and 400 °C. For the untreated wood sample, degradation occurs in two main steps that correspond, respectively, to the decomposition of hemicellulose (200–300 °C, $T_{max1} = 286.3$ °C) and cellulose (300–400 °C, $T_{max2} = 346.5$ °C). The thermal degradation of lignin has no obvious step in the TG curve because it covers a large temperature interval with

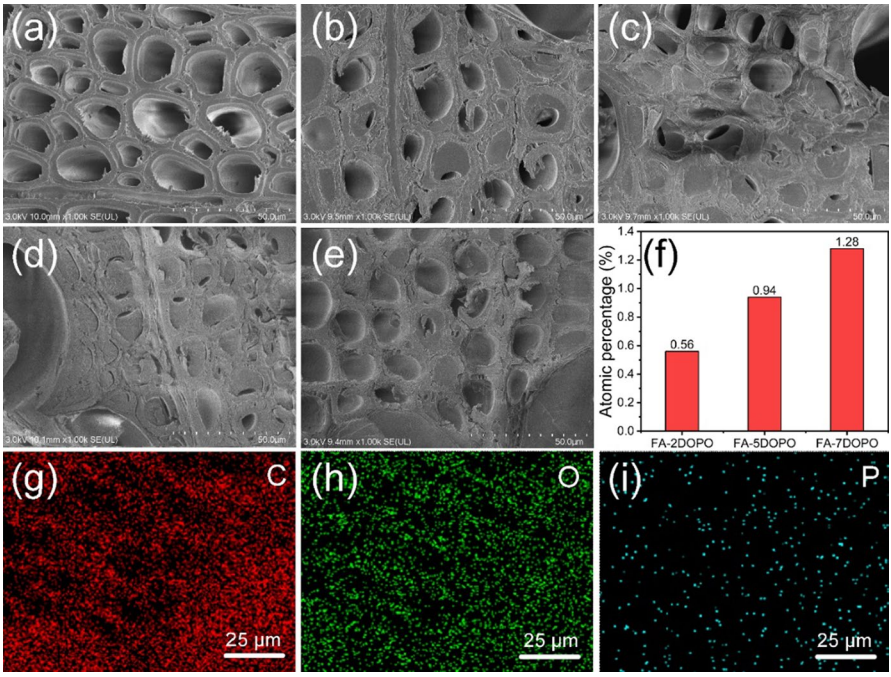

Fig. 5 SEM images of **a** untreated, **b** FA, **c** FA-2DOPO, **d** FA-5DOPO, and **e** FA-7DOPO samples. **f** Atomic percentage of phosphorus in FA-DOPO samples. Elemental mapping of **g** carbon, **h** oxygen, **i** phosphorus for **e** FA-7DOPO sample. The uniform distribution of P in the wood structure indicates the homogeneous dispersion of DOPO within wood structure

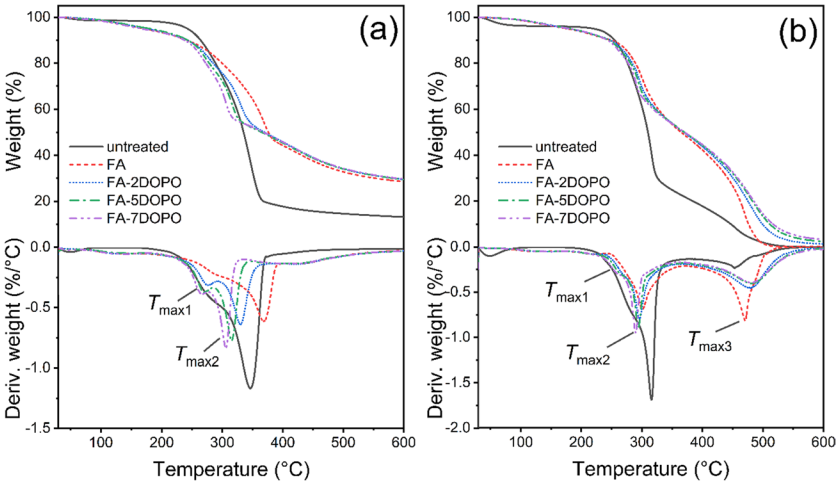

Fig. 6 TG (upper) and dTG (below) curves of the untreated and treated wood samples in **a** nitrogen and **b** oxygen atmosphere. Furfurylation endows wood with high thermal stability. The addition of DOPO can enhance the residue char yields of furfurylated wood

Table 1 TG data of the untreated and treated wood samples in nitrogen and oxygen atmosphere

Sample	Nitrogen			Oxygen			
	T_{max1} (°C)	T_{max2} (°C)	Residue (%)	T_{max1} (°C)	T_{max2} (°C)	T_{max3} (°C)	Residue (%)
Untreated	286.3	346.5	13.15	285.3	315.9	453.4	0
FA	288.8	368.9	28.47	278.7	301.2	470.8	0.19
FA-2DOPO	276.4	329.6	29.48	269.8	296.1	479.8	1.35
FA-5DOPO	271.1	315.6	29.47	263.9	294.5	481.8	2.48
FA-7DOPO	266.1	305.9	29.63	260.1	289.5	481.0	3.24

slow rate (Dong et al. 2020a). The T_{max1} and T_{max2} of furfurylated wood shift to higher temperatures, compared to the untreated wood sample. This result accords with our previous studies (Dong et al. 2020a; Liu et al. 2022), which confirmed that FA polymer has good thermal stability and, in turn, improves the thermal stability of wood. The weight residue of furfurylated wood is much higher than that of untreated wood, which could be caused by the high carbon content and the thermal stability of the FA polymers (Wang and Yao 2006). In addition, the bulking effect of furfurylation can increase the cell wall density, which could promote char formation during the thermal degradation. Clearly, the incorporation of DOPO into furfurylated wood decreases T_{max1} and T_{max2}, with the larger the amount added, the greater the reduction. This decreasing tendency could be due to the catalyzed dehydration of wood components by the phosphorus-containing organic compounds derived from DOPO (Qin et al. 2011).

In contrast to degradation in nitrogen, under an oxygen atmosphere, the thermo-oxidative degradation of hemicellulose and cellulose in untreated wood mainly occurs between 200 °C and 350 °C; this shift is due to oxygen. As temperature rises, a new apparent degradation stage occurs between 370 °C and 550 °C, with a T_{max3} of 453.4 °C. This stage is related to the thermal-oxidative decomposition of the char residues (Shen et al. 2009). Compared to untreated wood, all treated wood samples have a much lower weight loss during the first degradation stage, resulting from the formation of a larger amount of char residue. The presence of DOPO promotes the thermal pyrolysis of furfurylated wood during the first degradation stage, while restricting the thermal-oxidative decomposition of the char residue. As a result, the weight residue of furfurylated wood with DOPO under an oxygen atmosphere gradually rises with increasing amounts of DOPO. It is higher than that of DOPO-free furfurylated wood. These results indicate that the incorporation of DOPO into the furfurylation system can enhance the residue char yields of furfurylated wood.

Combustion behavior of the untreated and treated wood

The combustion behavior of untreated, FA, and FA-7DOPO samples under atmospheric conditions is illustrated in Fig. S3. When directly exposed to a flame, the untreated wood sample ignited quickly and burned intensely. The FA sample displayed a longer burning time. However, the degree of flaming of the FA sample was

more intense than that of untreated wood. Remarkably, the addition of DOPO inhibits flaming and reduces the burning time compared to the FA sample. Both the FA and FA-DOPO samples had more char residue than untreated wood.

Cone calorimetry tests were performed on untreated and treated wood samples to quantitatively study their combustion behavior. Figure 7 shows the HRR, THR, SPR, and THR of all samples, and their detailed data are listed in Table 2. In the HRR curves of all samples, two principal peaks are observed. The first peak is related to the ignition of volatile pyrolysis products after an initial heating period. Then, the heat release decreases as the char layer starts to build up. Later, a second peak occurs when the char layer breaks down (Ira et al. 2020). Compared to the untreated wood, the TTI of furfurylated wood is higher, while the HRR, SPR, EHC, and MAHRE of furfurylated wood are lower, indicating that furfurylated wood releases more combustible gas, contributing to fire propagation (Fitzer et al. 1969). This finding was also reported in previous studies (Kong et al. 2018; Sangregorio et al. 2020; Zhang et al. 2022c), suggesting that furfurylation has a negative effect on the flame retardancy of wood. After combustion, the untreated sample generates a little fragmentary, gray ash, while the FA sample yields a compact char skeleton with a substantial weight residue, consistent with the TG results and visual examination (Fig. 7e). Although the char residue is greater for furfurylated wood, the other flame-retardant parameters of furfurylated wood need to be improved.

It is apparent that the addition of DOPO reduces the HRR (both HRR peaks), THR, TSR, and MAHRE of furfurylated wood and improves the char residue yield. As the DOPO addition increases, the THR and MAHRE of treated wood are reduced. When the amount of DOPO is 7%, the total heat release is reduced by 37.4% compared with the furfurylated wood and is comparable with untreated wood. Table S2 lists the results of previous research in which the properties of furfurylated wood improved by different fire retardants were studied. Due to the high loading of FA polymer, the heat release of furfurylated wood is dramatic. It is confirmed that the addition of phosphorus-based flame retardants can reduce the heat release

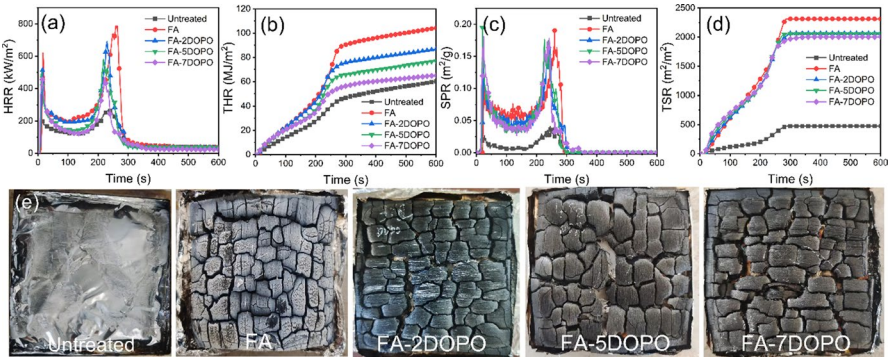

Fig. 7 Combustion behavior of untreated and treated wood samples: **a** HRR; **b** THR; **c** SPR; **d** TSR; **e** photographs of char residue after the cone test. FA sample exhibits much higher HRR and SPR than that of the untreated sample, while the addition of DOPO reduces the HRR, THR and TSR of furfurylated wood

Table 2 Cone calorimetry data of the untreated and treated wood samples

Sample	TTI (s)	First HRR peak (kW/m^2)	Second HRR peak (kW/m^2)	MAHRE (kW/m^2)	THR (MJ/m^2)	TSR (m^2/m^2)	Weight residue (%)	EHC (MJ/kg)
Untreated	11	196.6	267.9	162.1	60.4	476.8	11.2	12.3
FA	19	619.6	787.4	316.3	104.3	2313.9	29.8	13.2
FA-2DOPO	16	528.4	688.9	270.1	86.9	2063.5	35.4	11.3
FA-5DOPO	15	503.5	577.8	252.2	77.4	2055.7	35.5	11.4
FA-7DOPO	14	461.0	468.1	238.2	65.3	1997.0	37.1	11.6

of furfurylated wood effectively. However, the TSP is not dramatically reduced with increasing DOPO content. Compared to the FA sample, the samples treated with DOPO have a greater amount of char residue and less gray ash on the surface, indicating the positive effect of DOPO on char formation and thermal stability. During combustion, the decomposition of DOPO generates the phosphorus-containing acid, which catalyzes the carbonization reaction and the endothermic dehydration of the wood sample (including the wood components and FA polymer) (Liu et al. 2021). The phosphorus-rich, tough, char residue inhibits the spread of heat to the inner matrix (Wang et al. 2016). Therefore, it can be concluded that the addition of DOPO has a positive effect on promoting the flame retardancy of the furfurylated wood, but its effect on the smoke suppression needs to be improved further.

Condensed phase analysis

Figure 8 shows FE-SEM images and elemental distributions of the char residues of FA and FA-7DOPO samples from the cone calorimeter test. For the FA sample, numerous pores are formed (Fig. 8a), indicating an instantaneous burst of heat and

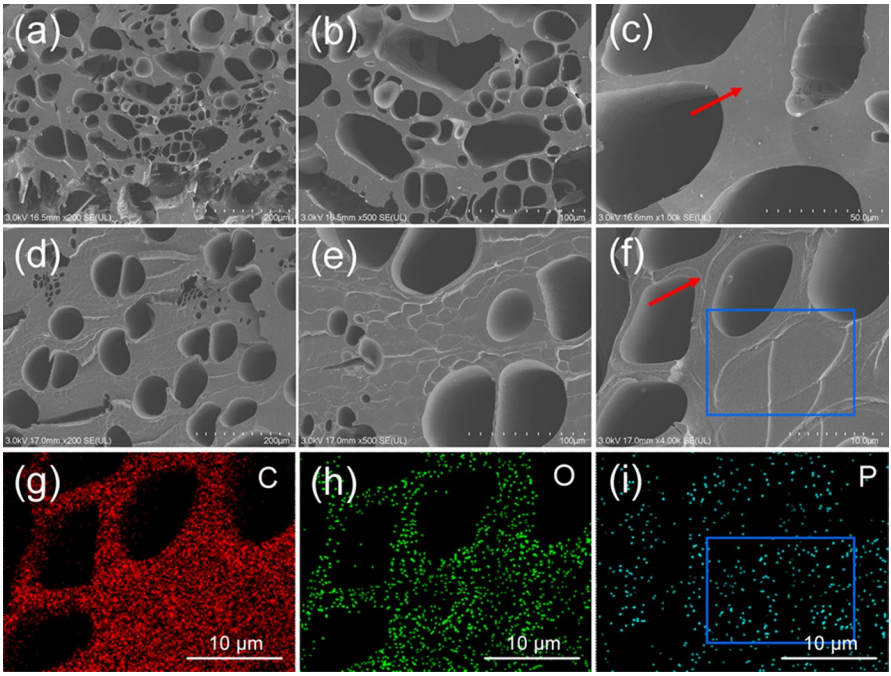

Fig. 8 FE-SEM images and elemental distributions of the char residues from the cone calorimeter test. **a** FA sample, **b** and **c** are magnified images of (**a**); **d** FA-7DOPO sample, **e** and **f** are magnified images of (**d**); **g–i** are the element distribution of C, O, and P for image (**f**), respectively. Compared to the FA sample, wood's cellular structure is retained well in the FA-7DOPO sample (arrow area). The distribution of P element is uniform both in the cell wall structure and the filled lumen in the char residue of the FA-7DOPO sample (square area)

smoke during combustion. The cellular structure of wood is damaged during the pore and char formation (Fig. 8b, c), which could be due to the highly viscous FA polymer, induced by the combustion process, coating the wood structure, and generating an expanded char residue (Zhang et al. 2022a). In contrast, the FA-7DOPO sample exhibits a less porous structure (Fig. 8d) and a clearly defined wood cellular structure (Fig. 8e, f). Meanwhile, the distribution of P is uniform both in the cell wall structure and the filled lumens (Fig. 8i). These results indicate that DOPO can penetrate the wood cell wall with the assistance of FA and that it interacts with the FA polymer to form a stable network in the wood structure. The fire-retardant effect of DOPO could promote char formation and inhibit the diffusion of oxygen and the escape of pyrolysis products. Consequently, the pore structure of the FA-7DOPO sample, caused by the release of heat and smoke, is less apparent than in the FA sample. The char residue is also greater than that of the FA sample (37.1% vs. 29.8%, Fig. 7e).

The char residues of the FA and FA-DOPO samples were further studied by XPS, as shown in Fig. 9. The XPS spectra indicate that the char residues are mainly composed of C and O. The additional P element appears in the char residue of the FA-DOPO sample, representing the presence of phosphorus oxides (Niu et al. 2022). The C1s spectra are deconvoluted into three sub-peaks corresponding to C–C/C=C, C–O/C–P, and C=O, respectively (Cai et al. 2023; Dong et al. 2019). Compared to the FA sample, the FA-DOPO sample has a higher relative content of C–O/C–P (18.2% vs. 12.8%), which explains the higher thermal oxidation resistance due to the addition of DOPO (Bhakare et al. 2023; Wang et al. 2022). These results reveal that

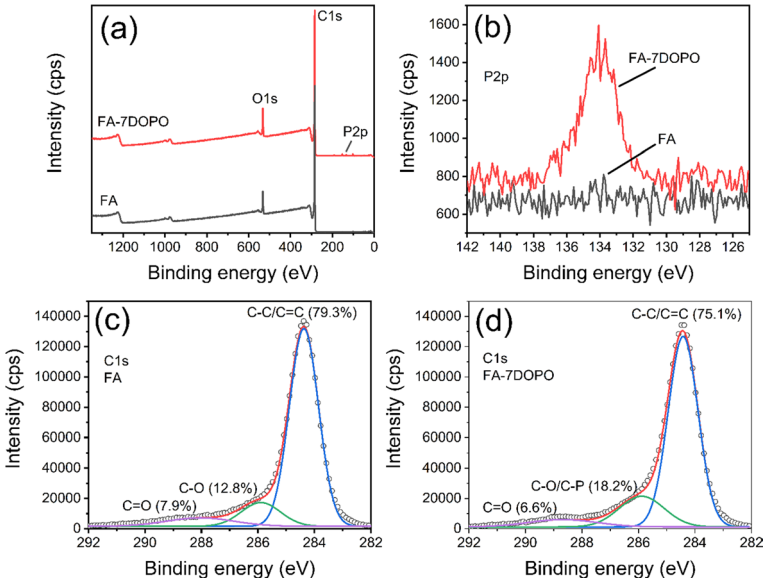

Fig. 9 XPS spectra of char residues for FA and FA-7DOPO samples. **a** full scan, **b** high-resolution spectra of P2p, and a high-resolution spectrum of C1s for **c** FA sample and **d** FA-7DOPO sample. The addition of DOPO results in a higher relative content of C–O/C–P than that of the FA sample

Table 3 ASE and leachability of treated wood samples

Wood samples	Leachability (%)	ASE (%)
FA	0.3 ± 0.1	77.1 ± 1.0
FA-2DOPO	0.7 ± 0.1	70.9 ± 2.4
FA-5DOPO	0.8 ± 0.1	71.3 ± 2.7
FA-7DOPO	0.6 ± 0.3	71.6 ± 1. 7

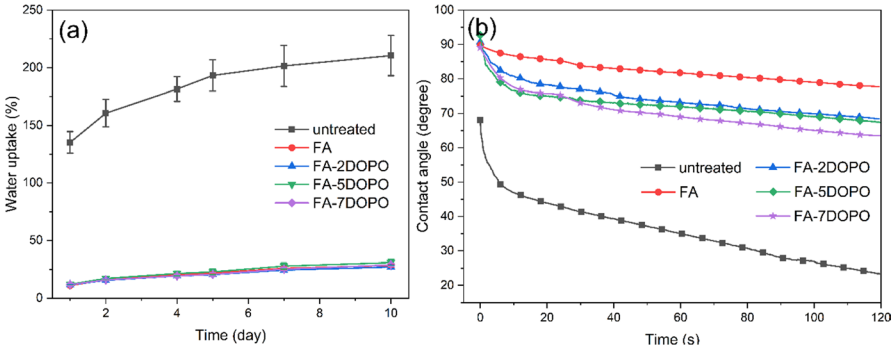

Fig. 10 **a** Water uptake and **b** dynamic wettability of untreated and treated wood samples. Furfurylated wood has much higher water resistance and lower wettability than untreated wood. The addition of DOPO decreases the contact angle of furfurylated wood to some extent

P in DOPO promotes char formation in furfurylated wood during combustion, and more char residue plays an essential fire-retardant role in the condensed phase.

Physical and mechanical properties of the treated wood samples

The leaching resistance of fire retardants is an important indicator when evaluating the durability of the flame retardancy of wood because the majority of conventional fire retardants are water-soluble and are easily leached by moisture (Lin et al. 2021). Furfurylation can inhibit the leaching of fire retardants by reducing the moisture absorption of wood. In addition, the FA can react with DOPO and form robust chemical bonding, which could further fix DOPO into the wood structure. Therefore, the leachability of treated wood samples is negligible (Table 3).

To evaluate the effect of DOPO on the physical and mechanical properties of furfurylated wood, the dimensional stability, water uptake, MOR, MOE, and hardness were tested. As shown in Table 3, the ASE of the FA sample reaches 77% due to the high WPG value. The addition of DOPO results in a slight decrease in ASE; a possible reason for this could be that the reaction between DOPO and FA reduces the impact of the FA polymer on the cell wall to some extent. Compared to the untreated wood sample, all treated wood samples exhibit a distinct reduction in water uptake capacity (Fig. 10a). After 10 days water immersion, the WU of untreated wood is 210%, while the WU of all treated samples is approximately 30%. The good water

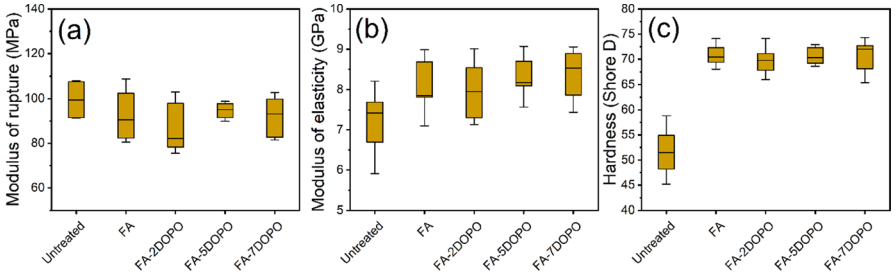

Fig. 11 **a** MOR, **b** MOE, and **c** surface hardness of untreated and treated wood samples. The DOPO has negligible effect on the mechanical properties of furfurylated wood

resistance of the treated wood samples is caused by the bulking effect and the hydrophobicity of the FA polymer, which is beneficial to the dimensional stability and leach resistance of treated wood. As shown in Fig. 10b, the contact angle of the FA sample gradually decreases as a function of time but is much higher than that of the untreated sample, indicating the low wettability of furfurylated wood. The addition of DOPO reduces the contact angle to some extent during the whole time, and this decreasing trend is exaggerated with the increasing amount of DOPO.

Figure 11 displays the mechanical properties of the untreated and treated wood samples. The average MOR and MOE values of the untreated wood sample are 99 MPa and 7.4 GPa, respectively. After furfurylation, the MOR is decreased by 7%, while MOE is increased by 11.8%, which is consistent with previous studies (Dong et al. 2015; Sejati et al. 2017). The hardness of the FA sample is 36.5% higher than the untreated one. The MOR, MOE, and hardness values of furfurylated wood samples in the presence of DOPO were almost the same as the FA sample, indicating the negligible effect of DOPO on the mechanical properties of furfurylated wood.

Conclusion

In the present study, DOPO was used as a fire retardant to improve the flame retardancy of furfurylated wood. SEM and FTIR results indicate the successful incorporation of DOPO, with a homogeneous dispersion within the wood structure. In addition, a covalent bond could be formed between the FA polymer and DOPO. Compared to untreated wood, furfurylated wood has a much higher heat and smoke release during combustion. With an increase in the concentration of DOPO, the heat release of furfurylated wood is substantially reduced and comparable to untreated wood. Additionally, DOPO can promote char formation in furfurylated wood and inhibit the diffusion of oxygen and the escape of pyrolysis products. Meanwhile, the addition of DOPO has little effect on the physical and mechanical properties of furfurylated wood. Nevertheless, DOPO does not suppress smoke production, so this aspect requires further investigation, such as introducing other flame retardancy components that contain nitrogen, boron, and silicon and form a stable network with the FA polymer.

Supplementary Information The online version contains supplementary material available at https://doi.org/10.1007/s00226-023-01513-2.

Acknowledgements This work was supported by Postdoctoral Science Foundation of Zhejiang Province (ZJ2022144), National Natural Science Foundation of China (32001253), Natural Science Foundation of Jiangsu Province (BK20200790), and Natural Science Foundation of Zhejiang Province (LQ19C160014).

Author contributions YD: Methodology, Investigation, Writing-original draft. ZF, YY and JS: Methodology, Investigation. MH: Writing—review & editing, Supervision. XZ: Resources, Supervision. JL: Project administration.

Funding Open Access funding provided by Aalto University.

Declarations

Conflict of interests The authors declare no competing interests.

References

Barsberg ST, Thygesen LG (2017) A combined theoretical and FT-IR spectroscopy study of a hybrid poly(furfuryl alcohol): Lignin material: basic chemistry of a sustainable wood protection method. ChemistrySelect 2:10818–10827. https://doi.org/10.1002/slct.201702104

Bertarione S, Bonino F, Cesano F, Jain S, Zanetti M, Scarano D, Zecchina A (2009) Micro-FTIR and micro-raman studies of a carbon film prepared from furfuryl alcohol polymerization. J Phys Chem B 113:10571–10574. https://doi.org/10.1021/jp9050534

Bhakare MA, Lokhande KD, Bondarde MP, Dhumal PS, Some S (2023) Dual functions of bioinspired, water-based, reusable composite as a highly efficient flame retardant and strong adhesive. Chem Eng J 454:140421. https://doi.org/10.1016/j.cej.2022.140421

Buonocore E, Häyhä T, Paletto A, Franzese PP (2014) Assessing environmental costs and impacts of forestry activities: a multi-method approach to environmental accounting. Ecol Model 271:10–20. https://doi.org/10.1016/j.ecolmodel.2013.02.008

Cai Y, Zhang J, Yue B, Wu J, Yu Y, Hu J, Qu J, Tian D (2023) Robust, anti-icing, and anti-fouling superhydrophobic coatings enabled by water-based coating solution. Prog Org Coat 182:107700. https://doi.org/10.1016/j.porgcoat.2023.107700

Cao X, Zhao W, Huang J, He Y, Liang X, Su Y, Wu W, Li RKY (2021) Interface engineering of graphene oxide containing phosphorus/nitrogen towards fire safety enhancement for thermoplastic polyurethane. Compos Commun 27:100821. https://doi.org/10.1016/j.coco.2021.100821

Dhumal PS, Lokhande KD, Bondarde MP, Bhakare MA, Some S (2022) Heat resistive, binder-free 3D-dough composite as a highly potent flame-retardant. J Appl Polym Sci 139(20):52146. https://doi.org/10.1002/app.52146

Dong Y, Yan Y, Zhang S, Li J, Wang J (2015) Flammability and physical-mechanical properties assessment of wood treated with furfuryl alcohol and nano-SiO_2. Eur J Wood Prod 73(4):457–464. https://doi.org/10.1007/s00107-015-0896-y

Dong Y, Zhang W, Hughes M, Wu M, Zhang S, Li J (2019) Various polymeric monomers derived from renewable rosin for the modification of fast-growing poplar wood. Compos Part B 174:106902. https://doi.org/10.1016/j.compositesb.2019.106902

Dong Y, Ma E, Li J, Zhang S, Hughes M (2020a) Thermal properties enhancement of poplar wood by substituting poly(furfuryl alcohol) for the matrix. Polym Compos 41:1066–1073. https://doi.org/10.1002/pc.25438

Dong Y, Wang K, Li J, Zhang S, Shi SQ (2020b) Environmentally benign wood modifications: a review. ACS Sustain Chem Eng 8(9):3532–3540. https://doi.org/10.1021/acssuschemeng.0c00342

Ehmcke G, Pilgård A, Koch G, Richter K (2017) Topochemical analyses of furfuryl alcohol-modified radiata pine (*Pinus radiata*) by UMSP, light microscopy and SEM. Holzforschung 71(10):821–831. https://doi.org/10.1515/hf-2016-0219

Esteves B, Nunes L, Pereira H (2011) Properties of furfurylated wood (*Pinus pinaster*). Eur J Wood Prod 69(4):521–525. https://doi.org/10.1007/s00107-010-0480-4

Falco G, Guigo N, Vincent L, Sbirrazzuoli N (2018) Opening furan for tailoring properties of bio-based poly(furfuryl alcohol) thermoset. Chemsuschem 11(11):1805–1812. https://doi.org/10.1002/cssc.201800620

Fitzer E, Schaefer W, Yamada S (1969) The formation of glasslike carbon by pyrolysis of polyfurfuryl alcohol and phenolic resin. Carbon 7(6):643–648. https://doi.org/10.1016/0008-6223(69)90518-1

Grinins J, Biziks V, Rizikovs J, Irbe I, Militz H (2021) Evaluation of water related properties of birch wood products modified with different molecular weight phenol-formaldehyde oligomers. Holzforschung 75(10):908–916. https://doi.org/10.1515/hf-2020-0235

Hadi YS, Mulyosari D, Herliyana EN, Pari G, Arsyad WOM, Abdillah IB, Gérardin P (2021) Furfurylation of wood from fast-growing tropical species to enhance their resistance to subterranean termite. Eur J Wood Prod 79(4):1007–1015. https://doi.org/10.1007/s00107-021-01676-4

Hill CAS (2006) Wood modification: chemical, thermal and other processes. Wiley, Chichester. https://doi.org/10.1002/0470021748

Ira J, Hasalová L, Šálek V, Jahoda M, Vystrčil V (2020) Thermal analysis and cone calorimeter study of engineered wood with an emphasis on fire modelling. Fire Technol 56(3):1099–1132. https://doi.org/10.1007/s10694-019-00922-9

Jiang J, Li J, Gao Q (2015) Effect of flame retardant treatment on dimensional stability and thermal degradation of wood. Constr Build Mater 75:74–81. https://doi.org/10.1016/j.conbuildmat.2014.10.037

Jin S, Qian L, Qiu Y, Chen Y, Xin F (2019) High-efficiency flame retardant behavior of bi-DOPO compound with hydroxyl group on epoxy resin. Polym Degrad Stab 166:344–352. https://doi.org/10.1016/j.polymdegradstab.2019.06.024

Kherroub DE, Belbachir M, Lamouri S (2015) Study and optimization of the polymerization parameter of furfuryl alcohol by Algerian modified clay. Arabian J Sci Eng 40(1):143–150. https://doi.org/10.1007/s13369-014-1512-x

Kong L, Guan H, Wang X (2018) In situ polymerization of furfuryl alcohol with ammonium dihydrogen phosphate in poplar wood for improved dimensional stability and flame retardancy. ACS Sustainable Chem Eng 6(3):3349–3357. https://doi.org/10.1021/acssuschemeng.7b03518

Kundu CK, Wang X, Rahman MZ, Song L, Hu Y (2020) Application of chitosan and DOPO derivatives in fire protection of polyamide 66 textiles: towards a combined gas phase and condensed phase activity. Polym Degrad Stab 176:109158. https://doi.org/10.1016/j.polymdegradstab.2020.109158

Li W, Liu M, Wang H, Yu Y (2020) Fabrication of highly stable and durable furfurylated wood materials. Part I Process Optim Holzforschung 74(12):1135–1146. https://doi.org/10.1515/hf-2019-0286

Lin C, Karlsson O, Martinka J, Rantuch P, Garskaite E, Mantanis GI, Jones D, Sandberg D (2021) Approaching highly leaching-resistant fire-retardant wood by in situ polymerization with melamine formaldehyde resin. ACS Omega 6(19):12733–12745. https://doi.org/10.1021/acsomega.1c01044

Liu D, Ji P, Zhang T, Lv J, Cui Y (2021) A bi-DOPO type of flame retardancy epoxy prepolymer: Synthesis, properties and flame-retardant mechanism. Polym Degrad Stab 190:109629. https://doi.org/10.1016/j.polymdegradstab.2021.109629

Liu X, Liu J, Dong Y, Hughes M, Wu M, Li J (2022) Evaluation of natural weathering and thermal degradation behavior of furfurylated bamboo strips at different weight percent gain. Eur J Wood Prod 80(2):289–299. https://doi.org/10.1007/s00107-021-01784-1

Lu J, Jiang P, Chen Z, Li L, Huang Y (2021) Flame retardancy, thermal stability, and hygroscopicity of wood materials modified with melamine and amino trimethylene phosphonic acid. Constr Build Mater 267:121042. https://doi.org/10.1016/j.conbuildmat.2020.121042

Ma Y, Geng X, Zhang X, Wang C, Chu F (2019) Synthesis of DOPO-g-GPTS modified wood fiber and its effects on the properties of composite phenolic foams. J Appl Polym Sci 136(2):46917. https://doi.org/10.1002/app.46917

Marney DCO, Russell LJ (2008) Combined fire retardant and wood preservative treatments for outdoor wood applications: a review of the literature. Fire Technol 44(1):1–14. https://doi.org/10.1007/s10694-007-0016-6

Martin LS, Jelavić S, Cragg SM, Thygesen LG (2021) Furfurylation protects timber from degradation by marine wood boring crustaceans. Green Chem 23(20):8003–8015. https://doi.org/10.1039/D1GC01524A

Niu H, Ding H, Huang J, Wang X, Song L, Yu Y (2022) A furan-based phosphaphenanthrene-containing derivative as a highly efficient flame-retardant agent for epoxy thermosets without deteriorating thermomechanical performances. Chin J Polym Sci 40:233–240. https://doi.org/10.1007/s10118-022-2655-y

Ouyang B, Yin F, Li Z, Jiang J (2022) Study on the moisture-induced swelling/shrinkage and hysteresis of *Catalpa bungei* wood across the growth ring. Holzforschung 76:711–721. https://doi.org/10.1515/hf-2021-0222

Peng W, Nie S, Xu Y, Yang W (2021) A tetra-DOPO derivative as highly efficient flame retardant for epoxy resins. Polym Degrad Stab 193:109715. https://doi.org/10.1016/j.polymdegradstab.2021.109715

Pin JM, Guigo N, Vincent L, Sbirrazzuoli N, Mija A (2015) Copolymerization as a strategy to combine epoxidized linseed oil and furfuryl alcohol: The design of a fully bio-based thermoset. Chemsuschem 8(24):4149–4161. https://doi.org/10.1002/cssc.201501259

Principe M, Martínez R, Ortiz P, Rieumont J (2000) The polymerization of furfuryl alcohol with p-toluenesulfonic acid: Photocross-linkeable feature of the polymer. Polímeros 10(1):8–14. https://doi.org/10.1590/S0104-14282000000100004

Qian L, Ye L, Qiu Y, Qu S (2011) Thermal degradation behavior of the compound containing phosphaphenanthrene and phosphazene groups and its flame retardant mechanism on epoxy resin. Polymer 52(24):5486–5493. https://doi.org/10.1016/j.polymer.2011.09.053

Qiu JF, Zhang MQ, Rong MZ, Wu SP, Karger-Kocsis J (2013) Rigid bio-foam plastics with intrinsic flame retardancy derived from soybean oil. J Mater Chem A 1(7):2533–2542. https://doi.org/10.1039/C2TA01404A

Salmeia KA, Gaan S (2014) An overview of some recent advances in DOPO-derivatives: chemistry and flame retardant applications. Polym Degrad Stab 113:119–134. https://doi.org/10.1016/j.polymdegradstab.2014.12.014

Samanta A, Höglund M, Samanta P, Popov S, Sychugov I, Maddalena L, Carosio F, Berglund LA (2022) Charge regulated diffusion of silica nanoparticles into wood for flame retardant transparent wood. Adv Sustain Syst 6:2100354. https://doi.org/10.1002/adsu.202100354

Sangregorio A, Muralidhara A, Guigo N, Thygesen LG, Marlair G, Angelici C, de Jong E, Sbirrazzuoli N (2020) Humin based resin for wood modification and property improvement. Green Chem 22(9):2786–2798. https://doi.org/10.1039/C9GC03620B

Sejati PS, Imbert A, Gérardin-Charbonnier C, Dumarçay S, Fredon E, Masson E, Nandika D, Priadi T, Gérardin P (2017) Tartaric acid catalyzed furfurylation of beech wood. Wood Sci Technol 51(2):379–394. https://doi.org/10.1007/s00226-016-0871-8

Shen DK, Gu S, Luo KH, Bridgwater AV, Fang MX (2009) Kinetic study on thermal decomposition of woods in oxidative environment. Fuel 88(6):1024–1030. https://doi.org/10.1016/j.fuel.2008.10.034

Thomas A, Moinuddin K, Zhu H, Joseph P (2021) Passive fire protection of wood using some bio-derived fire retardants. Fire Saf J 120:103074. https://doi.org/10.1016/j.firesaf.2020.103074

Thygesen LG, Beck G, Nagy NE, Alfredsen G (2021) Cell wall changes during brown rot degradation of furfurylated and acetylated wood. Int Biodeterior Biodegrad 162:105257. https://doi.org/10.1016/j.ibiod.2021.105257

Ünver H, Öktem Z (2013) Controlled cationic polymerization of furfuryl alcohol. Eur Polym J 49(5):1023–1030. https://doi.org/10.1016/j.eurpolymj.2013.01.025

Wang H, Yao J (2006) Use of poly (furfuryl alcohol) in the fabrication of nanostructured carbons and nanocomposites. Ind Eng Chem Res 45(19):6393–6404. https://doi.org/10.1021/ie0602660

Wang X, Zhang Q (2004) Synthesis, characterization, and cure properties of phosphorus-containing epoxy resins for flame retardance. Eur Polym J 40(2):385–395. https://doi.org/10.1016/j.eurpolymj.2003.09.023

Wang J, Qian L, Huang Z, Fang Y, Qiu Y (2016) Synergistic flame-retardant behavior and mechanisms of aluminum poly-hexamethylenephosphinate and phosphaphenanthrene in epoxy resin. Polym Degrad Stab 130:173–181. https://doi.org/10.1016/j.polymdegradstab.2016.06.010

Wang K, Meng D, Wang S, Sun J, Li H, Gu X, Zhang S (2022) Impregnation of phytic acid into the delignified wood to realize excellent flame retardant. Ind Crop Prod 176:114364. https://doi.org/10.1016/j.indcrop.2021.114364

Weng Z, Senthil T, Zhuo D, Song L, Wu L (2016) Flame retardancy and thermal properties of organoclay and phosphorous compound synergistically modified epoxy resin. J Appl Polym Sci 133(18):43367. https://doi.org/10.1002/app.43367

Yang T, Zhang K, Mei C, Ma E, Cao J (2022) Effects of furfurylation on interactions between moisture sorption and humidity conditioning of wood. Wood Sci Technol 56:703–720. https://doi.org/10.1007/s00226-022-01375-0

Yao J, Wang H, Liu J, Chan KY, Zhang L, Xu N (2005) Preparation of colloidal microporous carbon spheres from furfuryl alcohol. Carbon 43(8):1709–1715. https://doi.org/10.1016/j.carbon.2005.02.014

Zhang J, Duan H, Zou J, Cao J, Wan C, Zhang C, Ma H (2021) A DOPO derivative constructed by sulfaguanidine and thiophene toward enhancing fire safety, smoke suppression, and mechanical properties of epoxy resin. Macromol Mater Eng 306(12):2100569. https://doi.org/10.1002/mame.202100569

Zhang L, Ran Y, Peng Y, Wang W, Cao J (2022a) Combustion behavior of furfurylated wood in the presence of montmorillonite and its char characteristics. Wood Sci Technol 56(2):623–648. https://doi.org/10.1007/s00226-022-01369-y

Zhang L, Wang W, Chen J, Cao J (2022b) Dimensional stability and decay resistance of clay treated, furfurylated, and clay-reinforced furfurylated poplar wood. Holzforschung 76(3):256–267. https://doi.org/10.1515/hf-2021-0110

Zhang L, Zhang W, Peng Y, Wang W, Cao J (2022c) Thermal behavior and flame retardancy of poplar wood impregnated with furfuryl alcohol catalyzed by boron/phosphorus compound system. Ind Crop Prod 176:114361. https://doi.org/10.1016/j.indcrop.2021.114361

Zhou Y, Lin Y, Tawiah B, Sun J, Yuen RKK, Fei B (2021) DOPO-decorated two-dimensional mxene nanosheets for flame-retardant, ultraviolet-protective, and reinforced polylactide composites. ACS Appl Mater Interfaces 13(18):21876–21887. https://doi.org/10.1021/acsami.1c05587

Žlahtič-Zupanc M, Lesar B, Humar M (2018) Changes in moisture performance of wood after weathering. Construc Build Mater 193:529–538. https://doi.org/10.1016/j.conbuildmat.2018.10.196

Authors and Affiliations

Youming Dong[1,4] · Zhenyu Fu[1] · Yutao Yan[2] · Jingbo Shi[1] · Mark Hughes[3] · Xianxu Zhan[4] · Jianzhang Li[1]

✉ Mark Hughes
mark.hughes@aalto.fi

✉ Xianxu Zhan
jszx@dhwooden.com

[1] Co-Innovation Center of Efficient Processing and Utilization of Forest Resources, College of Materials Science and Engineering, Nanjing Forestry University, Nanjing, China

[2] School of Chemical and Material Engineering, Zhejiang A&F University, Hangzhou, China

[3] Wood Material Technology, Department of Bioproducts and Biosystems, Aalto University, Espoo, Finland

[4] Dehua Tubao New Decoration Material Co., Ltd, Huzhou, China